5-2019

The Effect of Cortical Remodeling on Bone Stiffness in White-tailed Deer Proximal Humerus

Jack Nguyen
Winthrop University, jackthanghanguyen@gmail.com

May, 2019

To the Dean of the Graduate School:

We are submitting a thesis written by Jack Nguyen entitled The Effect of Cortical Remodeling on Bone Stiffness in White-Tailed Deer Proximal Humerus. We recommend acceptance in partial fulfillment of the requirements for the degree of Master of Science in Biology.

[redacted]
Dr. Meir Barak DVM Ph.D., Thesis Advisor

[redacted]
Dr. Kristi Westover Ph.D., Committee Member

[redacted]
Dr. Julian Smith III Ph.D., Committee Member

[redacted]
Dr. Matthew Stern Ph.D., Committee Member

[redacted]
Dr. Adrienne McCormick, Dean, College of Arts & Sciences

[redacted]
Jack DeRochi, Dean, Graduate School

THE EFFECT OF CORTICAL REMODELING ON BONE STIFFNESS IN WHITE-TAILED DEER PROXIMAL HUMERUS

A Thesis

Presented to the Faculty

Of the

College of Arts and Sciences

In Partial Fulfillment

Of the Requirement for the Degree

Of

Master of Science

In the Department of Biology

Winthrop University

May 2019

by

Jack Nguyen

Abstract

Cortical remodeling is a process that replaces primary bone tissue with secondary or osteonal bone. Osteonal bone is characterized by the presence of secondary osteons or Haversian systems, which are cylindrical structures made up of concentric layers of bone tissue known as lamellae that surround a central canal. Remodeling is mediated by specialized cells known as osteoclasts and osteoblasts. These cells are signaled to selectively resorb and deposit secondary bone in specific areas by mechanical strain. Variations in the loading environment of bones can produce variations in secondary osteon size and morphology. This study investigated the effect of diverse *in vivo* loading (compression vs. tension) on the morphology of secondary osteons in the cranial (subjected to tensile loading) and caudal (subjected to compressive loading) aspects of the proximal humerus of white-tailed deer. Next, bone samples from the cranial and caudal aspects were mechanically tested in compression to find the stiffness of secondary osteonal bone in the proximal humerus of white-tailed deer. Finally, the bone samples were ashed and their composition was recorded (mineral, organic material and water content). Our histological results revealed significantly larger and more medially oriented secondary osteons with relatively smaller central canals in the cranial region. Nevertheless, Young's moduli and ash content were not significantly different between the cranial and caudal regions in all three principle axes (axial, radial and transverse). These results indicate that during bone remodeling - osteoclasts (bone resorbing cells) but not osteoblasts (bone depositing cells) are affected by the *in vivo* type and magnitude of loading. While the type of physiological stress affects bone resorption by osteoclasts (smaller cutting cones and consequently smaller secondary osteons under compression), bone deposition and mineralization by

osteoblasts doesn’t differ. Consequently, cortical bone compressive stiffness is not affected by the type of physiological stresses.

Acknowledgments

My sincerest thanks go to my thesis advisor, Dr. Meir Bark, whom I have had the pleasure of working with for nearly the past four years. Without his continued support and guidance, I would not be the student I am today. I will forever be grateful for the opportunity to have worked with Dr. Barak. I would also like to thank my other committee members, Dr. Matthew Stern, Dr. Julian Smith III and Dr. Kristi Westover, who have advised me throughout this process and graciously agreed to be my readers. Also thank you Dr. Glasscock, your flexibility and support this past year has meant so much to me.

A special thanks goes to the Winthrop Biology Department and the SC INBRE Program who have funded my research; both as an undergraduate and graduate student. Lastly, I would like to thank all the amazing students I have had the pleasure of working with in my 5 years at Winthrop: Arielle Kunde, Arielle Black, Benjamin Harrison, Michael DeLashmutt, Naima Jackson, Meha Patel, Nick Tucker, Emily Long and Ashley Graham. Thank you for all the great memories. I will cherish them always.

Table of Contents

List of Tables and Figures

Previous Research

Note – the following section describes my previous undergraduate work / results and is not an integral part of my graduate thesis. It appears here since the information is key for understanding my current graduate project.

During my undergraduate research we studied cortical bone remodeling of the proximal humerus from white-tailed deer. We prepared cross sections from four proximal humeri and examined them using a scanning electron microscopy (JSM-6010LA InTouchScope™, JEOL USA Inc). Our results showed that the cranial and caudal aspects of the proximal humerus demonstrated extensive remodeling, evident from the large number of secondary osteons (Figure 1). Our results also demonstrated a significant difference in secondary osteons (Haversian systems) and central canal morphology (Figure 2). Secondary osteons in the cranial region were larger, angled more medially and had relatively smaller central canals (Figure 2). One possible explanation for these results is that regions subjected to tension (cranial aspect of the proximal humerus) experience lower stress magnitudes compared to regions that are subjected to compression (caudal aspect of the proximal humerus). Regions of high stress will benefit from smaller resorption pits (i.e. less bone material is lost in every remodeling occurrence) and smaller resorption pits will lead to smaller secondary osteons. (Skedros et al. 1997). Previous studies have also revealed that the rate of remodeling (% of secondary osteons in a given cortical bone region) and the shape and size of secondary osteons in various bone locations are influenced from the type, magnitude and frequency of loading (Lanyon et al., 1979, Martin et al., 1996, Skedros et al., 2013, Keenan et al., 2017). Thus, my graduate research is aimed

to determine if this structural difference between the cranial and caudal aspects of the proximal humerus of white-tailed deer had an effect on the stiffness of cortical bone tissue.

Proximal Humerus Cross-Section Image from SEM

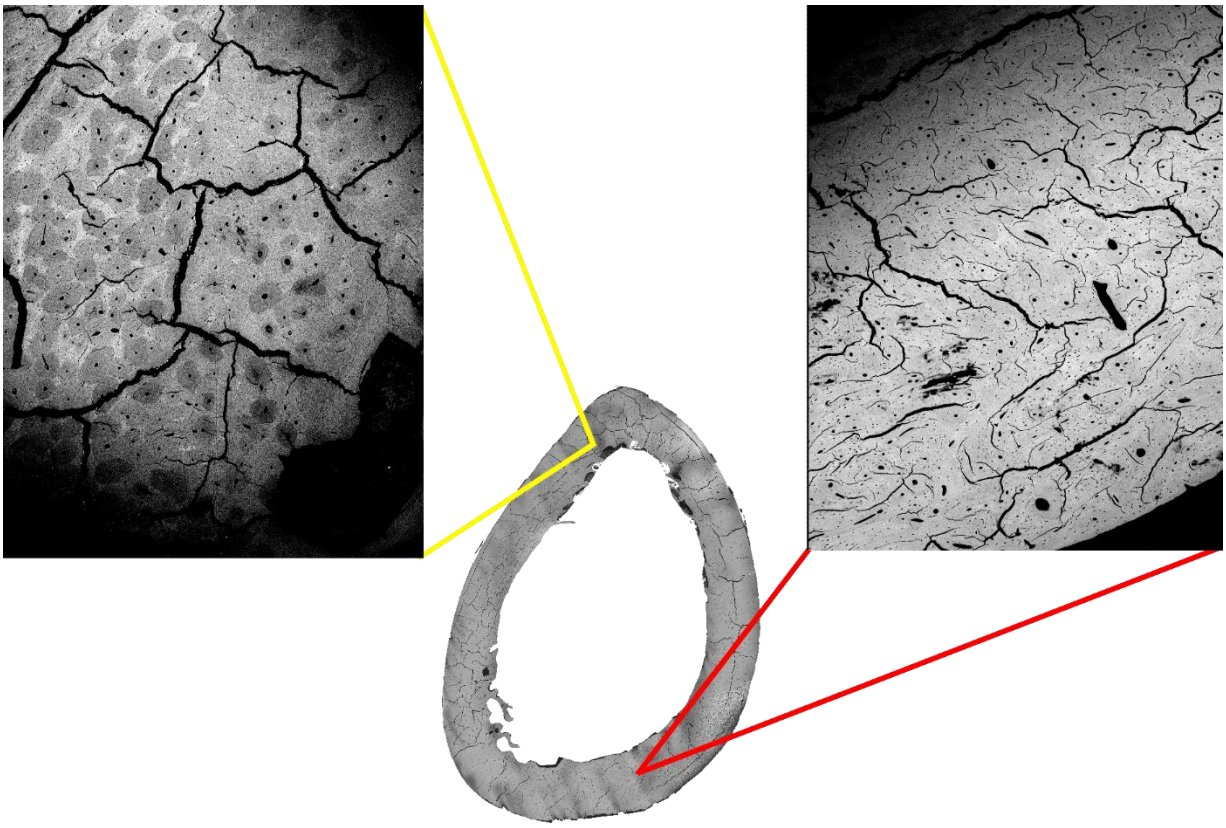

Figure 1. SEM image of a cross section cut from proximal humerus #1. Several images taken at x30 magnification were stitched together using PTGui version 10.0.16 to create a whole cross-section image. All histomorphometric measurements were taken from x40 magnification images from the cranial (left inset, yellow) and caudal (right inset, red) aspects of the proximal humerus. These x40 higher magnification images were used to quantify the extent of remodeling in each region.

Histomorphometric Data Summary

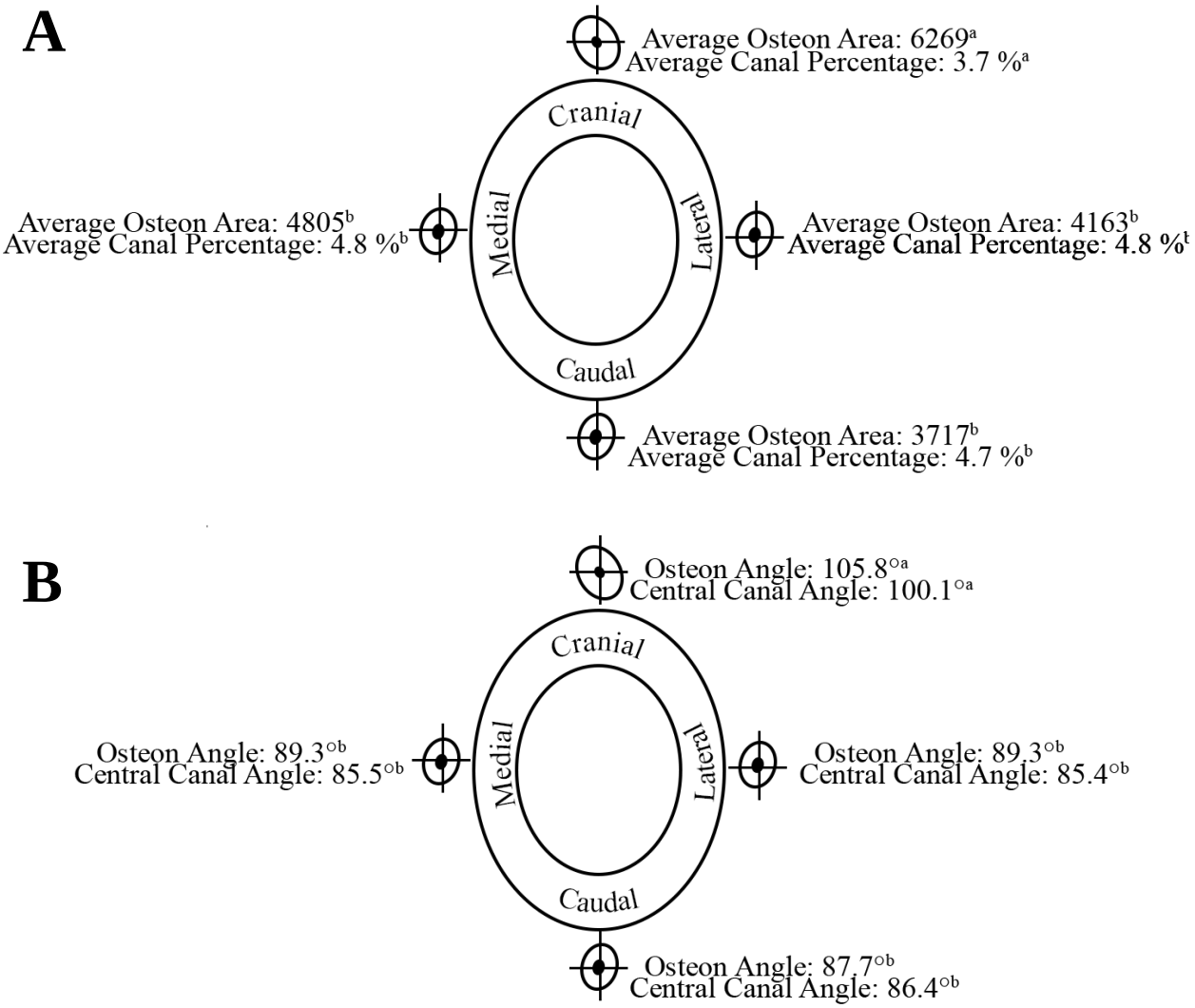

Figure 2. Histomorphometry of secondary osteons in the proximal humeri of white-tailed deer. Panel A: Average secondary osteon area (in pixels) and average relative central canal area (ratio between central canal area and secondary osteon area). Average secondary osteon area is significantly higher in the cranial aspect of the proximal humeri compared to the other regions. Average relative central canal area is significantly lower in the cranial aspect of the proximal humeri compared to the other regions. Panel B: Secondary osteon

and central canal angle relative to sagittal plane (lateral-medial). Structures with angles smaller than 90° are oriented craniolateral and structures with angles larger than 90° are oriented craniomedial., Similar to the results in panel A, the secondary osteons and their central canals in the cranial regions demonstrated a different behavior than all other regions – by being oriented craniomedially compared to craniolaterally in the medial, lateral and caudal aspects respectively.

Introduction

"Bone" is a term used to describe both the bone as an organ and the anisotropic material it is composed of. The material bone is a stiff, lightweight yet relatively elastic composite with seven hierarchical structure levels ranging from the nanoscale to the macroscale. In its lowest structural level, bone is composed of carbonated hydroxyapatite, the framework protein type I collagen, many other so-called non-collagenous proteins and water. In its highest hierarchical structure level, bone is made of two macroscopic architectures: dense cortical bone tissue (also called compact bone) and porous trabecular bone tissue (also called cancellous bone). The mechanical behavior of both cortical and trabecular bone tissues depend primarily on the properties of the material bone, especially its mineral content and porosity.

While bone is a mineralized stiff structure it is far from stagnant. As bones (the organ) are loaded daily, they are subjected to strains (deformations) and consequently they accumulate fatigue damage that will eventually form microcracks in the bone tissue. Bone remodeling is a biological mechanism that couples the resorption of old, usually damaged, bone tissue with the deposition of new bone material called osteoid. Thus, bone remodeling is a fundamental and critical process to the maintenance of healthy bone tissue in many vertebrate species. The process of bone remodeling produces concentric structures of bone lamellae known as secondary osteons or Haversian systems, which are a key microstructural component of cortical bone. As not all bone regions are loaded and strained equally, the outcome of bone remodeling (i.e. secondary osteons) is expected to vary in composition and morphology between regions that are subjected to different types and

magnitude of loading (compression vs. tension loads and high vs. low loads, respectively). This variation in bone tissue structure may potentially have a significant effect on the mechanical properties and function of bones (the organ). To address this structure-function relationship question, this study aimed to determine whether cortical bone tissue subjected to physiological tensile vs. compressive loading would demonstrate differences in secondary osteon morphology and mineralization, and consequently differences in compressive stiffness.

Bone Structure

The vertebrate skeletal system is made up of rigid organs (bones) which protect the internal organs, allow for locomotion, and maintain mineral homeostasis throughout the body (Patterson-Kane and Firth 2013). Bone material is a stiff, lightweight and relatively elastic composite material with a hierarchical structure. It is composed of a mineral phase known as hydroxyapatite, a framework protein called type I collagen, many other so-called non-collagenous proteins and water. The most significant organic component of bone material is made up of 90-95% collagen type I (Teitelbaum 2000). Collagen type I is a fibrillar structural protein that is formed from precursor molecules known as procollagen which consist of three intertwined polypeptide chains with long glycine and proline stretches (Currey 2002). These procollagen molecules associate in triplicate to form helical tropocollagen molecules that are approximately 300 nm in length with a diameter of roughly 1.5 nm. Tropocollagen molecules arrange side by side in a staggered fashion with small gaps between adjacent molecules to form collagen fibrils. These small gaps initially

contain water (osteoid state) but as bone tissue matures, the water is gradually replaced with hydroxyapatite crystals, a process called biomineralization (Timmons and Wall 1977). With time, the biomineralization process progresses, and hydroxyapatite crystals start to accumulate outside the gaps and throughout the collagen fibril, creating a mineralized collagen fibril. Increased mineralization has been shown to dramatically increase the overall stiffness and strength of the bone (Currey 1969).

The mechanical behavior of bone tissue is also dependent on its three-dimensional macro-architecture, and in particular the interplay between the outer cortical (compact) shell and the inner trabecular (cancellous) bone. These two bone macro-architectures can be distinguished mainly by their porosity, with compact bone being about 3-5% porous and trabecular bone being 40% to 90% porous (Bonucci 2000). Compact bone comprises the dense exterior layer of whole bones and is responsible for 80% of skeletal weight (Ott 2018). Trabecular bone is comparatively more porous and features a honeycomb like structure consisting of connected rods and plates known as trabeculae. The long bones of mammals such as the humerus or femur feature trabecular bone primarily near the epiphyses whereas the diaphysis is composed almost entirely of compact bone (Buckwalter et al., 1995). Cortical bone can be divided into two types: primary compact bone, which is the first bone tissue that is deposited de-novo in young animals (such as woven or fibrolamellar bone), and secondary compact bone. Secondary compact bone is the product of bone remodeling and it is characterized by the presence of structures known as secondary osteons or Haversian systems. These secondary osteons are cylindrical structures with a diameter of about 150 - 250 μm (depending on bone and species), which run close to parallel to the long axis of the bone. They are made of concentric sheets of mineralized

collagen fibers (lamellae) that wrap around a central canal through which blood vessels pass.

Bone Remodeling

Bone remodeling is a highly coordinated biological process consisting of osteoclasts (bone resorbing cells) and osteoblasts (bone depositing cells) working in unison to maintain bone homeostasis (Hadjidakis and Androulakis 2007). These two cell types are spatially arranged in temporary anatomical structures known as Basic Multicellular Units (BMUs), which feature osteoclasts in the front leading portion and osteoblasts in the tail portion (Praffit 1994). This arrangement ensures that bone resorption is properly coupled with deposition and facilitates progression through the phases of bone remodeling.

The bone remodeling sequence consists of several distinct phases: activation, resorption, reversal, formation and resting. The first phase of bone remodeling is known as the activation phase, and involves an initiating signal which is induced mechanical strain placed on the bone during physiological loading. These signals are perceived by osteocytes (former osteoblasts that are now embedded in the bone matrix) which under basal conditions secrete a growth factor (TGF-β) that inhibits osteoclast differentiation (Raggatt and Patridge 2010). Initiating signals induce osteocyte apoptosis thereby reducing the concentration of TGF-β and helping to promote osteoclastogenesis and the recruitment of osteoclasts to the remodeling site. Once recruited, osteoclasts polarize on the bone surface and form a specialized cell membrane structure consisting of several folds known as a ruffed border (Raggatt and Patridge 2010). This border forms an isolated environment

underneath the cell known as the “sealed zone” into which protons are secreted that break down the mineral component of bone (resorption phase) (Allen and Burr 2014). Resorption within sealed zones by osteoclasts can happen either on bone surfaces or within the bone tissue (Patterson-Kane and Firth 2013). Osteoclasts resorption on bone surfaces results in the formation of resorption pits otherwise known as Howship’s lacunae. Osteoclasts resorption within the bone tissue results in the formation of cutting cones. After resorption of the mineral component, the unmineralized collagen is then removed during the reversal phase of bone remodeling. In this phase, the collagen remnants are removed by specialized “reversal” cells derived from the osteoblast lineage. This sets the stage for the formation phase, in which osteoblasts are signaled to the resorption site by reversal cells and begin to secrete an organic matrix known as osteoid. This newly secreted osteoid is laid down in layers known as lamellae. On bone surfaces, lamellae are filling the resorption pits as groups of relatively flat structures called packets. Within the bone tissue, lamellae are filling the cutting cones in a concentric manner (from the periphery to the center), forming secondary osteons, and leaving the center void (central canals) for the formation of blood vessels. Finally, the newly deposited bone enters the resting phase in which the bone tissue continues to mineralize with hydroxyapatite crystals but is inactive in resorption or deposition. Following biomineralization, the newly laid bone tissue is left undisturbed until a new remodeling cycle is initiated.

Biomechanical Analysis of Bone Tissue

Stress is defined as the force applied to a structure per unit area and is obtained by dividing the force by the area over which it acts (Turner and Burr 1993). A proper definition of stress requires that both the orientation of the area and the direction of the force be described. When the applied force is perpendicular to the area over which it acts, the stress is said to be a "normal" stress. Normal stresses can be compressive – when the direction of loading is oriented toward the object, resulting in compression or tensile - when the direction of loading is oriented away from the object, resulting in elongation (Sedlin, 1965). When the applied force is not perpendicular to the area over which it acts, the stress is said to be a shear stress. Shear stress causes the two planes of a structure to slide past one another. Whole bones are subjected to all three forms of stress during *in vivo* loading. Strain is the consequence of stress and is defined as the change in length relative to the original length of the object (Morgan et al. 2018).

The stiffness of the bone organ is characterized by the relationship between the load and deformation the bone experiences (Dechow et al., 1993). Bone stiffness is typically quantified using a load-deformation curve that shows the amount of load needed to produce a certain change in length. This curve contains a linear portion known as the elastic region; the slope of which represents the stiffness of the structure. An important distinction must be made between the stiffness of whole bones such as the humerus or femur and the stiffness of bone tissue. The stiffness of bone tissue is an intrinsic property of the material and is independent of its geometry. Therefore, to measure the stiffness of bone tissue we need to normalize the load into stress and the deformation into strain. A stress-strain curve

for cortical bone tissue provides a value (Young's Modulus) that indicates the stiffness of the tissue itself (Morgan and Bouxsein 2008). In order to determine the Young's modulus of bone tissue, mechanical tests are conducted on prepared bone samples with a standardized geometry, such as a cube or a beam.

The Effect of Loading on Bone Remodeling

Bone remodeling is a highly adaptive process that allows bone to respond to changes in mechanical demand (Patterson-Kane and Firth 2013). For example, the humeri (forelimb) of quadrupeds such as deer primarily experience cranial to caudal bending during everyday movement (Figure 3). Therefore, the cranial aspect of the humerus is subjected primarily to tension and the caudal aspect of the humerus is subjected primarily to compression. It has been shown that regions of the bone loaded primarily in compression experience higher magnitudes of stresses when compared against regions loaded primarily in tension (Riggs et al., 1993). A previous study by Lanyton et al., (1979) quantified this discrepancy through the use of rosette strain gauges on the cranial and caudal cortices of sheep radii and found a peak locomotor stress ratio of 1.56 to 1 (caudal (compression) to cranial (tension)). Additionally, a higher degree of remodeling was also noted in the caudal cortices, suggesting that higher stresses cause more damage (microcracks) and stimulate more remodeling activity. Bone remodeling has been shown to produce microstructural variation in secondary osteon and central canal size based on different loading environments (Skedros et al., 2007). Regions subjected to compressive loads experience higher stress and thus would benefit from smaller resorption pits (i.e. less bone material is

lost during each remodeling event) and smaller resorption pits will in turn lead to smaller secondary osteons. (Skedros et al. 1997). Bones such as the femur or humerus that are loaded in cranio-caudal bending during locomotion have been shown to contain larger secondary osteons in regions that experience tensile stresses vs regions that experience compressive stresses (Skedros 2013). This variation in osteon size is thought to relate to the strain distribution across these regions which is perceived as a signal by the BMUs that then selectively resorb more or less bones in these regions.

Differing secondary osteon morphology in cortical bone can be studied using scanning electron microscopy (SEM) or circularly polarized light microscopy (CPL) and has been used as the basis for differentiating human bone from that of other mammals (Dominguez and Crowder, 2012). Polarized light microscopy is often used for a general analysis of secondary osteon features, whereas scanning electron microscopy is used for exact histomorphometric measurements (such as secondary osteonal area and shape) due to the higher resolution of the instrument.

Secondary osteons under CPL display various birefringence patterns (seen as peripheral rings around the central canal) based on lamellar structure and collagen fibril orientation that have been shown to correspond to load history (Skedros et al., 2009). These patterns are used as the basis for categorizing secondary osteons into distinct morphotypes which are distinguished based on the brightness of peripheral rings as they appear under polarized light. It has been observed that bone regions which primarily experience compressive loads, feature secondary osteons with collagen fibrils that run more obliquely to the transverse plane, thus producing brighter peripheral rings when compared against

regions that experience tensile stress (Skedros et al., 2013). Data such as osteon area, diameter, and circularity can all be obtained from SEM micrographs and are useful in determining the strain distribution across regions of the bone. In particular, the tension cortices of the deer calcaneus have been shown to contain larger more ellipsoid (less circular) osteons when compared against the tension cortices (Keenan et al., 2017).

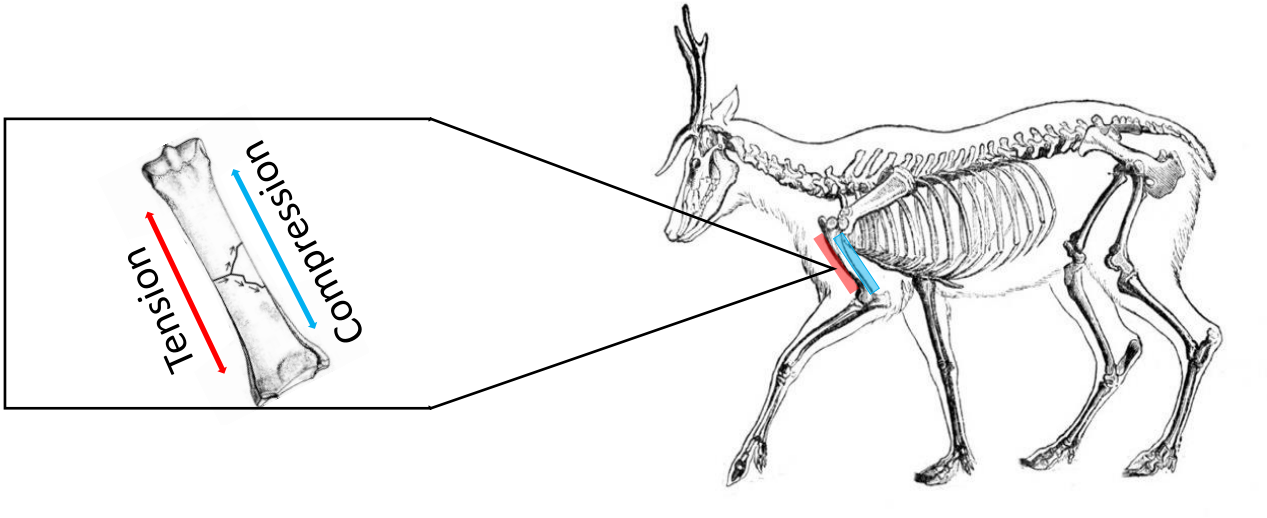

Figure 3. On the right: A schematic drawing of the white-tailed deer skeleton. Left humerus is highlighted (red/blue). On the left: Close up of the cranial and caudal aspects of the humerus. Red arrows indicate regions which experience primarily tensile stresses (cranial) and blue arrows indicated regions which experience compressive stresses (caudal). The lateral and medial aspects of the humerus lie along a neutral axis and experience comparatively lower amounts of both stress types.

Experiment Rationale

As stated above, secondary osteons vary in shape and size in response to the type of physiological loading (compression or tension) and the magnitude of loading (high vs, low stresses). These structural differences may have an effect on the mechanical properties (namely stiffness) of bone tissue. Yet to the best of my knowledge, no previous study has investigated the relationship between secondary osteons shape and morphology to their compressive stiffness. My hypothesis for this study is that cortical bone cubes from the caudal aspect of the proximal humerus that is subjected to compressive loads (and was shown to have smaller secondary osteons in my undergraduate project), will have greater stiffness in all three orthogonal directions.

This study compares the stiffness of cortical bone cubes from the cranial and caudal aspects of the proximal humerus in white-tailed deer (*Odocoileus virginianus*) by subjecting them to compression testing. Overall, 36 cubes will be tested from the cranial aspect, and 39 will be tested from the caudal aspect. Compression testing will be done on each cube in the axial, radial, and transverse orientations.

By quantifying differences in secondary osteonal size and morphology across separate regions of the proximal humerus and relating these to the mechanical properties (Young's Modulus) of the bone, we can potentially gain a better understanding of how the bone is loaded and which regions are most heavily stressed. This information has direct relevance to the study of fossils from extinct taxa, as their bony remains can imply how they have lived and moved. Additionally, mineral content, stiffness, and osteon size and morphology have been previously been used to differentiate between human and non-

human bone (Skedros et al., 2016). Measurements from this study could be used as a point of comparison in cases where it is necessary to distinguish human from non-human bone, or deer bone.

Materials and Methods

Bone Sample Preparation

Humeri from seven white-tailed deer were obtained from One Price Deer Processing Plant, York SC. Age and sex were undetermined, however all bones showed active growth plates indicating deer were juveniles whose bones were still in the growth phase. All soft tissue was removed, and humeri were stored in a -20°C freezer prior to cutting. All humeri were measured from most proximal to most distal ends and the proximal portions of each bone (between 10%-35% of bone length) were sectioned into approximately 3 cm thick segments using a hand-saw (Figure 4). Each segment was then further cut into four quadrants based on its anatomical orientation (cranial, caudal, lateral and medial). Next, the cranial and caudal quadrants were cut into 2x2x2mm cubes along the bone principle axes (axial, radial and transverse) using a low speed water-cooled diamond saw (TechCut 4 precision low speed saw, Allied Technologies). Thirty-six cubes were cut from the cranial aspect and thirty-nine cubes were cut from the caudal aspect. Cubes were stored in 1.5mL Eppendorf tubes containing paper soaked in saline solution with 8% chloroform. All samples were kept frozen at −20°C until testing. Each sample was thawed at 4°C in the same saline solution twenty-four hours prior to testing.

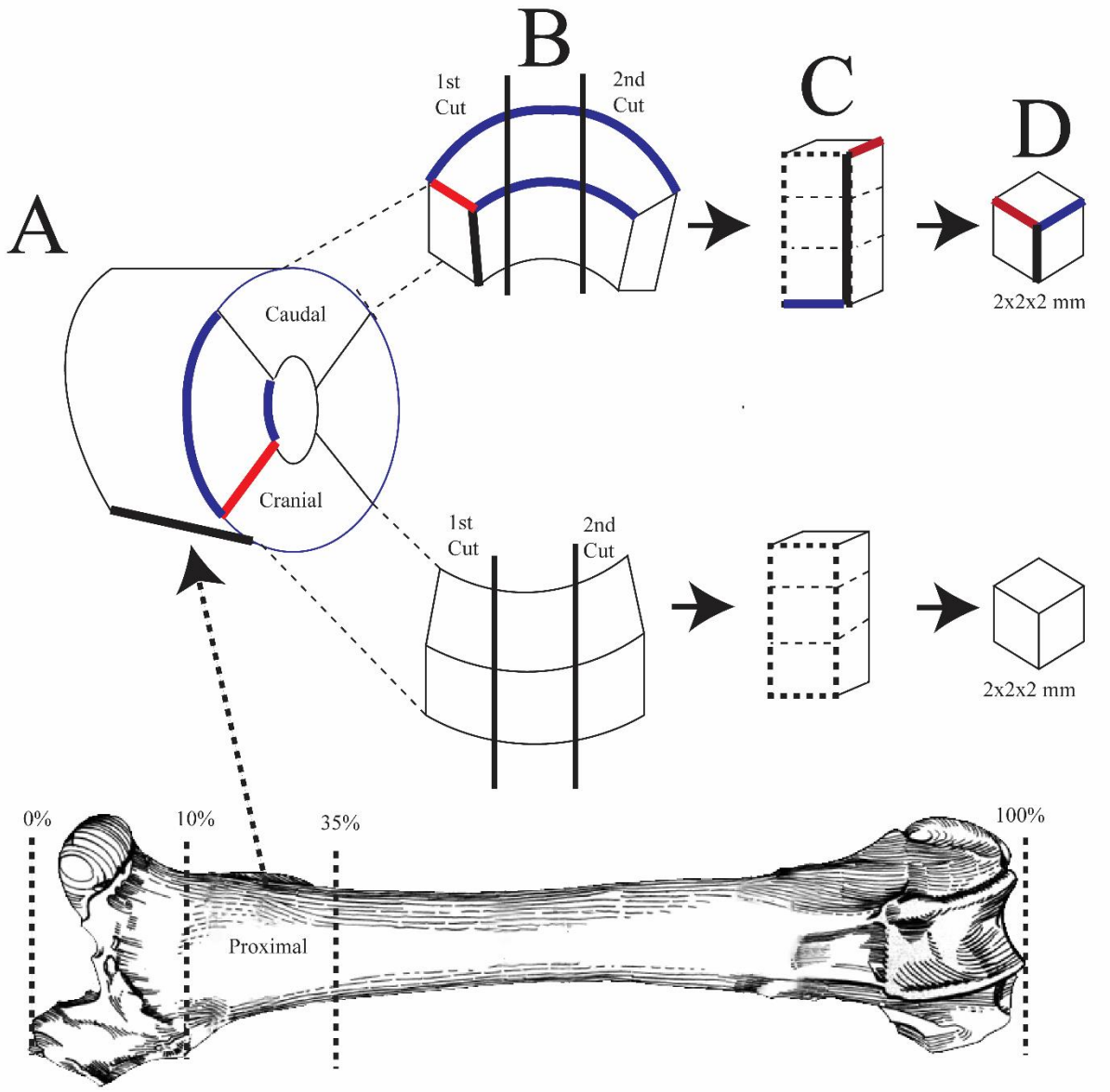

Figure 4. A schematic diagram of the sample preparation process. Initial cuts were made to remove the proximal region of each humeri (Denoted ‘A” in the figure). Subsequent cuts were then made along the axial direction of each sample in order to isolate cranial and caudal sections (Denoted ‘B” in the figure). Each orientation was then marked as follows; black = axial, blue = transverse, red = radial. Orientations were continually labeled

throughout the rest of the cutting process to allow for correct identification of each principal axis. Cranial and caudal sections were then cut into 2mm beams (Denoted ‘C” in the figure). Finally, 2x2x2mm cubes were prepared by cutting along the transverse plane of each beam (Denoted ‘D” in the figure).

Sample Imaging

Using a Nikon Eclipse E600 microscope with a camera, images were taken from the transverse plane of each cortical bone cube to determine the extent of remodeling in each sample cube (Figure 5). Any secondary osteons present (indicators of remodeling) would be visible on this plane as secondary osteons run perpendicular to the long axis of the bone. Eight samples (6 cranial and 2 caudal) were found to have trabecular bone present, most likely because these cubes were cut close to the endosteal surface of the proximal, an area that contains trabecular bone. Therefore, these sample were omitted.

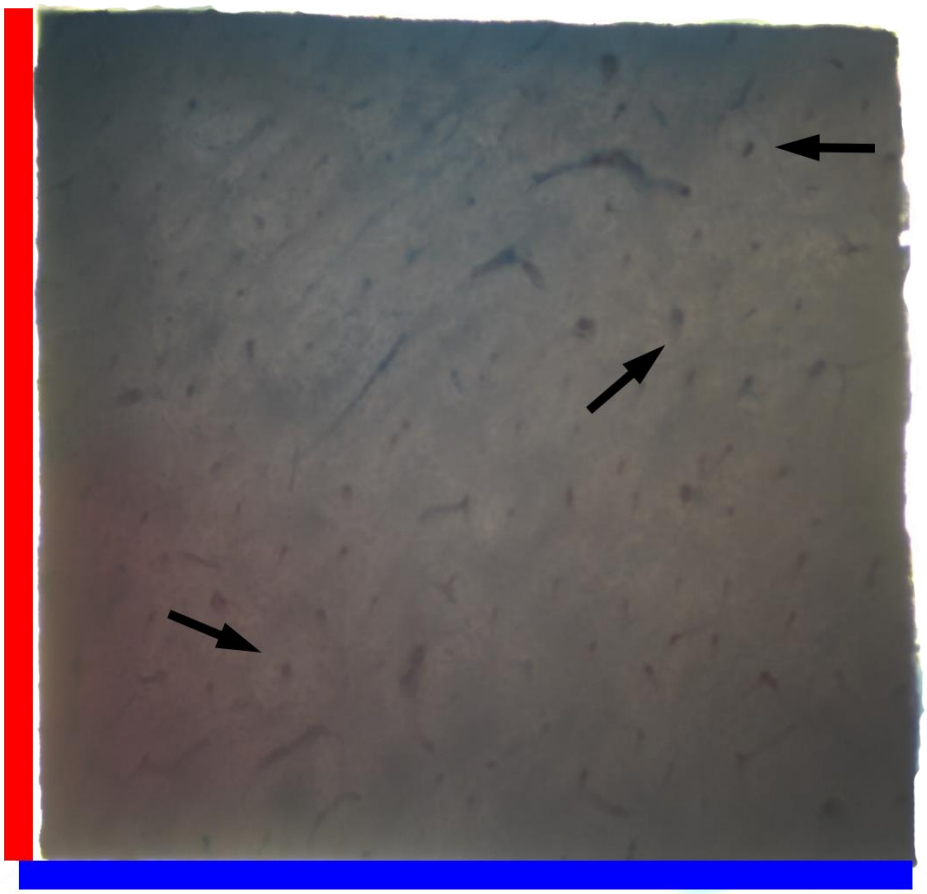

Figure 5. Picture of the radial-transverse plane when viewed under a Nikon Eclipse E600 microscope. Directions are indicated by the red (radial) and blue (transverse) lines. Images of each sample were taken in order to evaluate the extent of remodeling. Examples for secondary osteons (indicated by arrows) were used to confirm the amount of remodeling present in each sample and whether cubes contained trabecular bone.

Compression Testing

All cortical bone cubes were non-destructively tested in compression, within their elastic region, using an Instron 5942 universal testing machine (Instron Inc., USA), (Figure

6A). Each cube was tested three times, once in each of its principle orientations – axial, radial and transverse. Order of testing directions was alternated to prevent any possible effect of test order (i.e. the possibility that the orientation that is tested last is affected by the previous two tests). The tested cube was mounted in the orientation being tested on a stationary anvil with a thin layer of dental composite (Z250,3M ESPE, St. Paul, MN, USA). The Z250 3M composite material was used due to its stiffness value - around 11GPa ("3M, Filtek Z250 - Universal Restorative System," 1998), which is within the range of cortical bone stiffness values (Shahar et al., 2007) and because it does not irreversibly bond with the bone material and can be removed with no damage at the end of each experiment. The use of dental composite as a load-transfer layer was validated and used successfully in previous studies (Barrera et al., 2016; Shahar et al., 2007). Another thin layer of composite was applied to the upper anvil which was then manually lowered until contact was made with the surface of the sample. The addition of composite to both anvil faces helped to correct any surface incongruences as a result of the cutting process and minimize stress concentration and sheer stress, ensuring the sample was loaded primarily in compression (Figure 6C). Composite was then polymerized for 60s using a hand-held light-cure device (GadgetWorkz Wood-pecker 5 W). Prior to loading, 0.2 mL of saline solution containing 8% chloroform was added around the bone cube between the anvils to keep the bone wet during the experiment. As tests were short (about 35 s per cycle and about 6–7 min for an entire experiment), all cubes were kept wet throughout the testing process. After a small preload of 5 N was applied at the beginning of each testing cycle, load and deformation data were collected every 0.1 s (BlueHill 3 Software ®, Instron, USA). Bone samples were loaded at a rate of 50 $\mu m\ sec^{-1}$ until a max load of 140 N ensuring bone samples remained

within the elastic region and sustained no structural damage. A previous study (Kunde et al., 2018) tested in compression 2x2x2mm bone cubes from white-tailed deer humeri and femora in all three orthogonal orientations (axial, radial and transverse) up to 460 N (close to the system and load cell maximum capacity of 500 N). Their results demonstrated that at 460 N, the cortical bone samples demonstrated no evidence of damage. In addition, comparable techniques with the same experimental setup also demonstrated a lack of damage when bone samples were repeatedly loaded in a similar range of loads (Barak et al., 2008, 2009; Sharir et al. 2008; Barrera et al., 2016). Accordingly, we have concluded that a load of 140 N was far from the bone's yield point in all three orientations and thus within the elastic region. Each mounted sample was loaded ten cycles per test with the first seven cycles serving as preconditioning. Previous studies have shown improved reproducibility and precise stiffness results when using several conditioning cycles to achieve a viscoelastic steady state (Sedlin and Hirsch, 1966; Linde and Hvid, 1987; Zioupos and Currey, 1998; Ding et al., 2012). Load and deformation data were obtained from the final three load cycles in order to calculate the material stiffness (Young's Modulus). The eight cubes which contained trabecular bone were excluded from the final data analysis as outliers (more than 3 standard deviations from the mean). The difference between cranial and caudal bone material stiffness was analyzed using a two-tailed t-test with unequal variance; values smaller than 0.05 ($P<0.05$) were considered to be statistically significant.

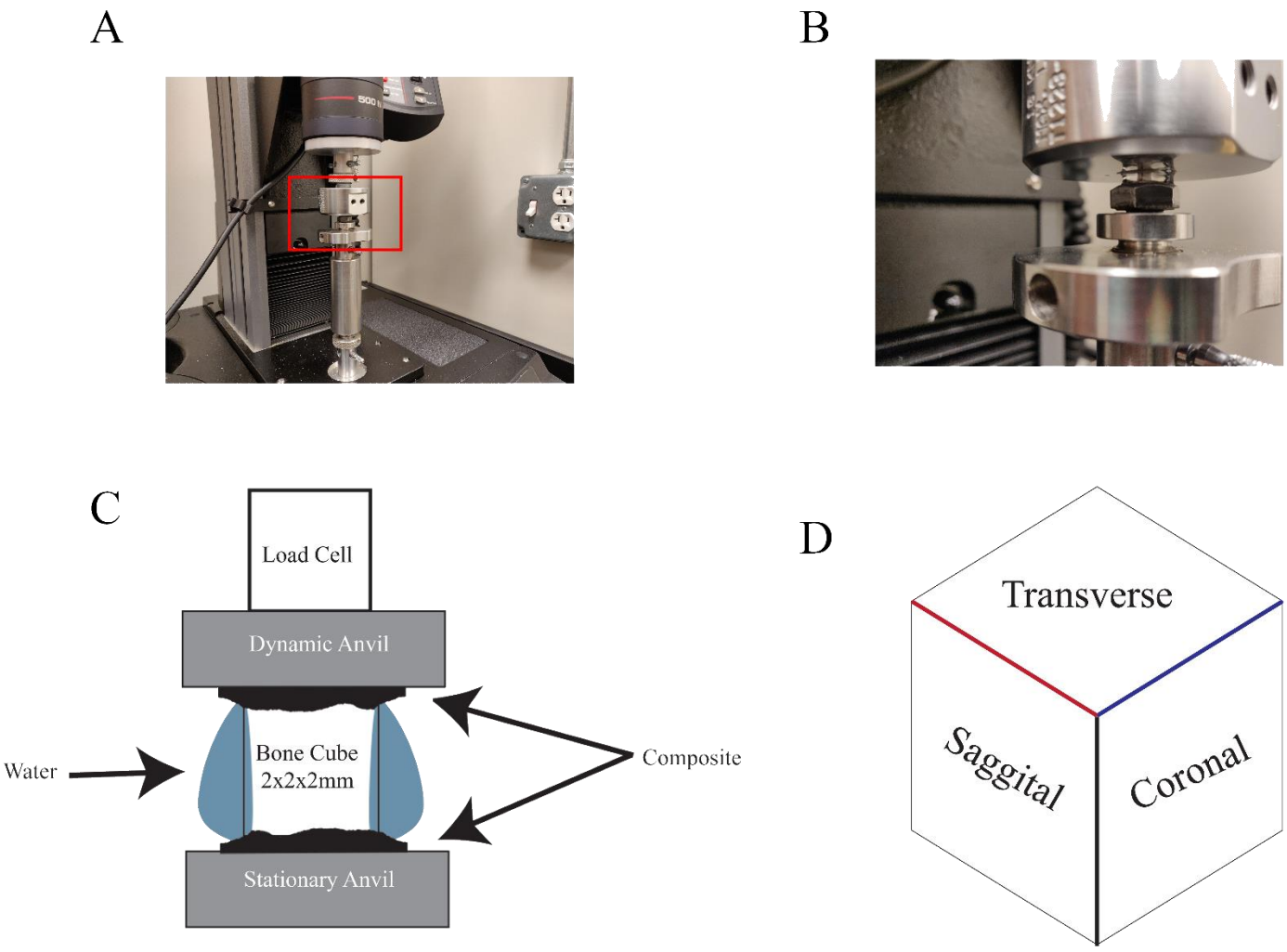

Figure 6. (A) Instron 5942 Universal testing machine shown in compression mode. The red frame outlines the higher magnification inset shown in panel 'B'. (B) A cube loaded in compression (sounded by water) between the two anvils. (C) A schematic diagram of a bone cube with all three orthogonal orientations labeled (black for axial, red for radial, and blue for transverse). (D) Schematic view of the mounted cube sample. A thin layer of

composite was applied to both anvil faces to minimize stress concentrations caused by any surface incongruencies.

Data Analysis for Compression Testing

Stress values for each cube were calculated for the last three loading cycles by determining the ratio of force applied by the Instron testing machine to the cross-sectional area of each sample. Strain was calculated using the ratio between the upper anvil's displacement and the distance between the anvils at the beginning of the experiment. Since this distance included the bone cube height and the thickness of the upper and lower composite layer, measurements were taken at the end of each experiment when the bone cube was removed, and composite thickness measurements were possible. Cortical bone material stiffness (Young's modulus) was determined manually from the linear, elastic region of the stress-strain curve (between 40 – 100 N). This was done by exporting the raw data files from the BlueHill 3 Software to Microsoft Excel and manually calculating the slope of the values within this range.

Microscope Section Preparation

While my Scanning Electron Microscopy images (undergraduate project, see Figure 1) clearly demonstrated that the cranial and caudal aspects of the proximal humeri were extensively remodeled, we decided to look at the cross-section of several bone cubes to verify that we have cut them from the right area and that they too were mostly remodeled.

After the compression testing was finished, six bone cubes (three from the cranial and three from the caudal groups) were decalcified in order to prepare them for paraffin embedding. Sections were used to confirm that bone cubes contained primarily secondary osteonal bone (Figure 7). Sample were rinsed in distilled water under slight agitation for thirty minutes to remove any surface debris. Samples were then placed in 50 mL cups containing 35 mL of 8% formic acid on a magnetic stirrer for seven days to allow for de-calcification. The acid solution was changed every twenty-four hours to prevent calcium buildup. Bone cubes were embedded in paraffin for histological sectioning using a previously established protocol (Porter et al., 2017). Each sample was first washed in 60% ethanol for a period of six and half hours, followed by subsequent one-hour washes in 70%, 80%, 95% and 100% ethanol. These dehydration steps were intended to remove all water from the bone samples to better facilitate paraffin infiltration process. Samples were then washed twice in xylene for thirty-minute before being added to paraffin (AMERAFFIN Tissue Embedding Medium, Baxter Scientific Products). Cubes were then placed in 50 mL glass beakers containing paraffin wax and heated to 60 °C in a Precision Economy Oven (Jouan Inc.). Samples were left in molten paraffin for a total of three hours with changes occurring at the 30-minute, 90-minute, 180- and 210-minute marks. Following paraffin infiltration, bone samples were embedded in plastic cassettes and stored for 48 hours in a 4°C refrigerator. Prior to sectioning, the surface of each wax block was placed in 4% potassium hydroxide for fifteen minutes to allow for more efficient sectioning via microtome. Sections were cut using a Leitz 1512 microtome and placed into a 45°C water bath before being transferred onto Superfrost Plus slides. Blocks were placed back into 4%

potassium hydroxide for fifteen-minute intervals following five minutes of sectioning or whenever samples began to chip on contact with microtome blade.

In order to de-paraffinize the slides for staining, each slide was placed in a Coplin staining jar and submerged in xylene for two minutes. This was repeated twice, afterwards the slides were transferred to Coplin jars containing 100% ethanol (2 x 1 min) and 95% ethanol (2 x 1 min). Lastly all slides were placed in 70% ethanol for one minute to fully de-paraffinize the sections. Slides were allowed to rest for five minutes to allow any excess alcohol to evaporate, and then submerged in distilled water for ten minutes. They were then transferred over to Coplin Jars containing hematoxylin and allowed to sit for fifteen minutes. Finally, all slides were removed and dipped four times in distilled water to rinse off any excess staining solution. Slides were placed under a Nikon eclipse E600 microscope and images were captured using a ProgRes C5 camera and ProgRes Mac CapturePro 2013 Software (Figure 7).

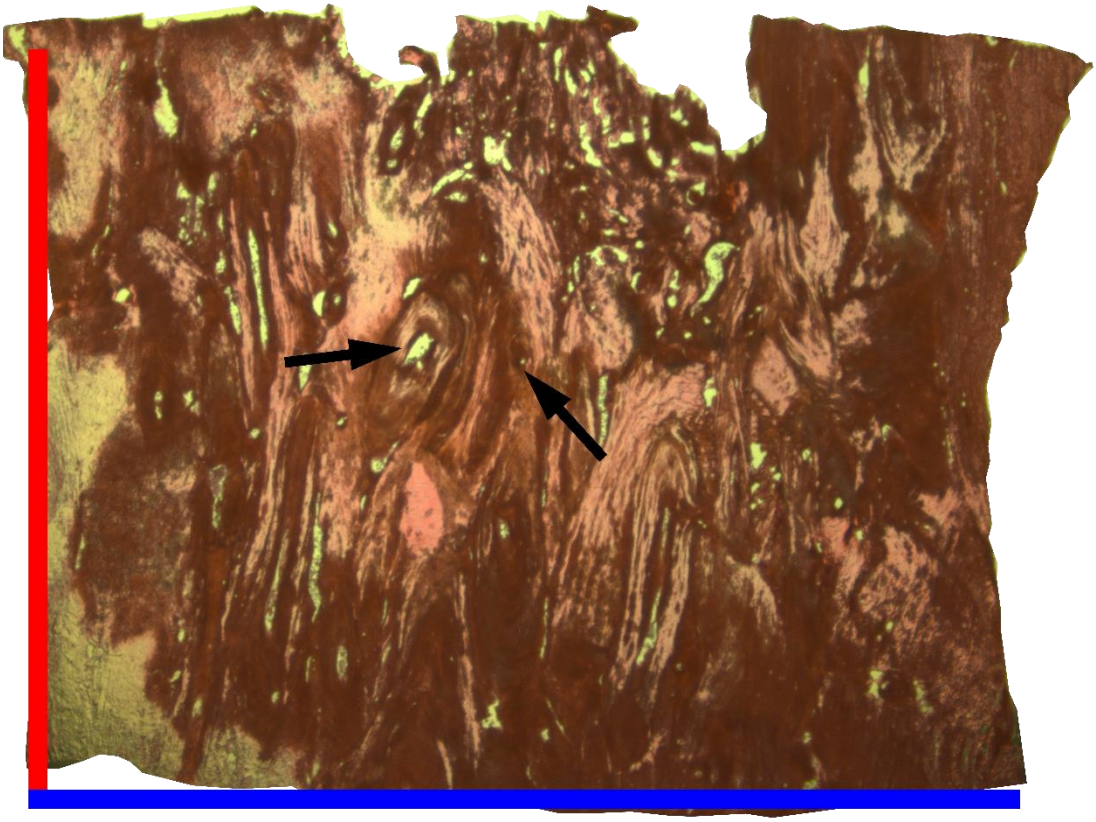

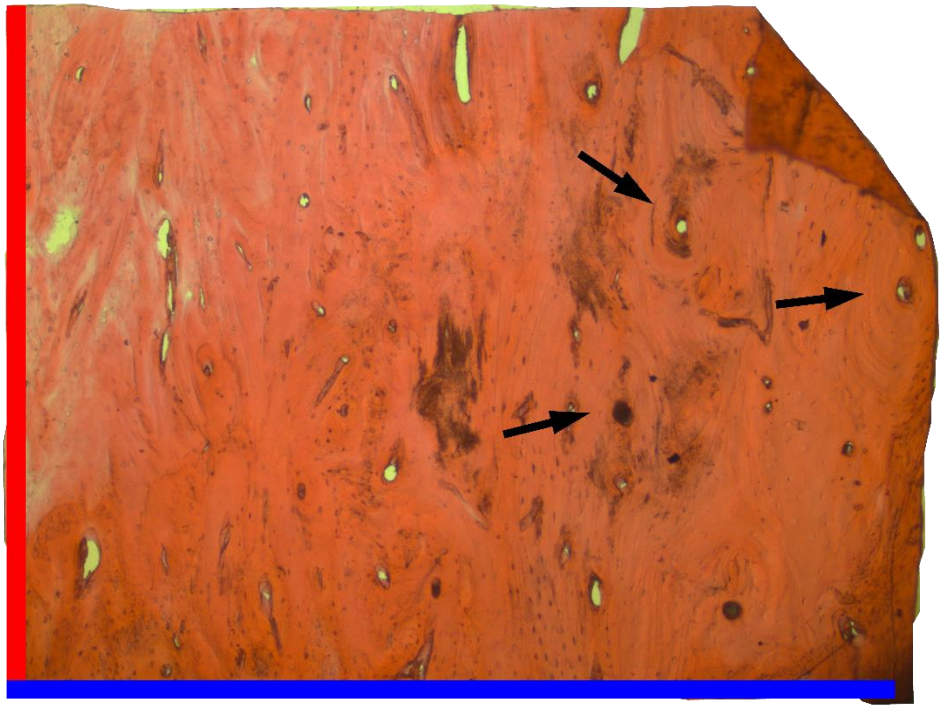

Figure 7. Histological transverse cross-sections of bone cube cut from the cranial (top) and the caudal aspects of the proximal humeri. The radial (red) and transverse (blue) orientations are indicated by the colored lines. Paraffin-embedded sections were used to confirm the presence of secondary osteons (several examples are indicated by arrows) showing that samples consisted primarily of secondary bone. Both cranial and caudal samples show similar degrees of remodeling. These finding are consistent with scanning electron and light-polarized micrographs that were taken during my undergraduate research which showed that both regions contained mostly secondary bone.

Bone Ashing and Mineral Content Analysis

Bone material from the cranial and caudal aspects of each proximal humerus was crushed into a fine powder in order to analyze the ratio of mineral, organic material and water. This bone material included previously tested cubes and leftover sections from cube preparation). Bone material was initially crushed using a hammer, before being ground using a mortar and pestle. The powder from each humerus was then divided into 70-100 mg samples and placed into 1.5 mL Eppendorf vials.

Two humeri (#5 and #3) lacked enough material from both aspects to test for mineral content (30-40 mg). Additionally, there was also an insufficient amount of material from the cranial aspect of humerus #7 material to be properly evaluated. The bone powder from each vial was weighed to determine the original weight and then placed into a ceramic boat. Next, the samples were heated to 100°C for three hours inside an Isotemp programmable forced-draft furnace (ThermoFisher Scientific) and their dry-weight was measured. The difference between initial-weight and dry-weight was calculated to

determine the amount of water present in each sample. All samples were then placed back into the furnace at 500°C for a period of fifteen hours. Each sample was then removed and re-weighed one last time. The amount of organic material present in each sample was calculated by subtracting the final mineral-weight from the previously recorded dry-weight. A two-tailed t-test with unequal variance was used to compare the water, organic material, and mineral weights of samples from the cranial vs the caudal regions of the proximal humeri. Values smaller than 0.05 ($P<0.05$) were considered to be statistically significant.

Results

Young's Modulus

Both cranial and caudal samples demonstrate transverse isotropy (Figure 8A and 8B) with Young's moduli values for the radial and transverse orientations non-significantly different from each other, but significantly lower than those of the axial orientation.

Average axial stiffness in the cranial aspect of the white-tailed deer proximal humerus was found to be 17.2 ± 4.2 GPa. Average axial stiffness in the caudal aspect of the white-tailed deer proximal humerus was found to be 18.5 ± 3.2 GPa (Table 1). Axial stiffness in the cranial and caudal aspects were found to be non-significantly different ($P>0.05$) (Figure 9A).

Average radial stiffness in the cranial aspect of the white-tailed deer proximal humerus was found to be 10.7 ± 2.4 GPa. Average radial stiffness in the caudal aspect of the white-tailed deer proximal humerus was found to be 10.0 ± 2.1 GPa. Radial stiffness in the cranial and caudal aspects were found to be non-significantly different ($P>0.05$) (Figure 9B).

Average transverse stiffness in the cranial aspect of the white-tailed deer proximal humerus was found to be 11.0 ± 2.4 GPa. Average transverse stiffness in the caudal aspect of the white-tailed deer proximal humerus was found to be 10.9 ± 1.8 GPa. Transverse stiffness in the cranial and caudal aspects were found to be non-significantly different ($P>0.05$) (Figure 9C).

In summary, both cranial and caudal aspects showed transverse isotropic behavior, and the overall stiffness per orientation was not significantly different when comparing the two regions (Figure 10)

	Cranial aspect (n=30) Average (SD) GPa	Caudal aspect (n=37) Average (SD) GPa
Axial	17.2 (4.2)	18.5 (3.2)
Radial	10.7 (2.4)	10.0 (2.1)
Transverse	11.0 (2.4)	10.9 (1.8)

Table 1. Average Young's moduli (standard deviation in parenthesis) in the axial radial and transverse orientations for samples tested from the cranial and caudal aspects of the proximal humerus in white-tailed deer.

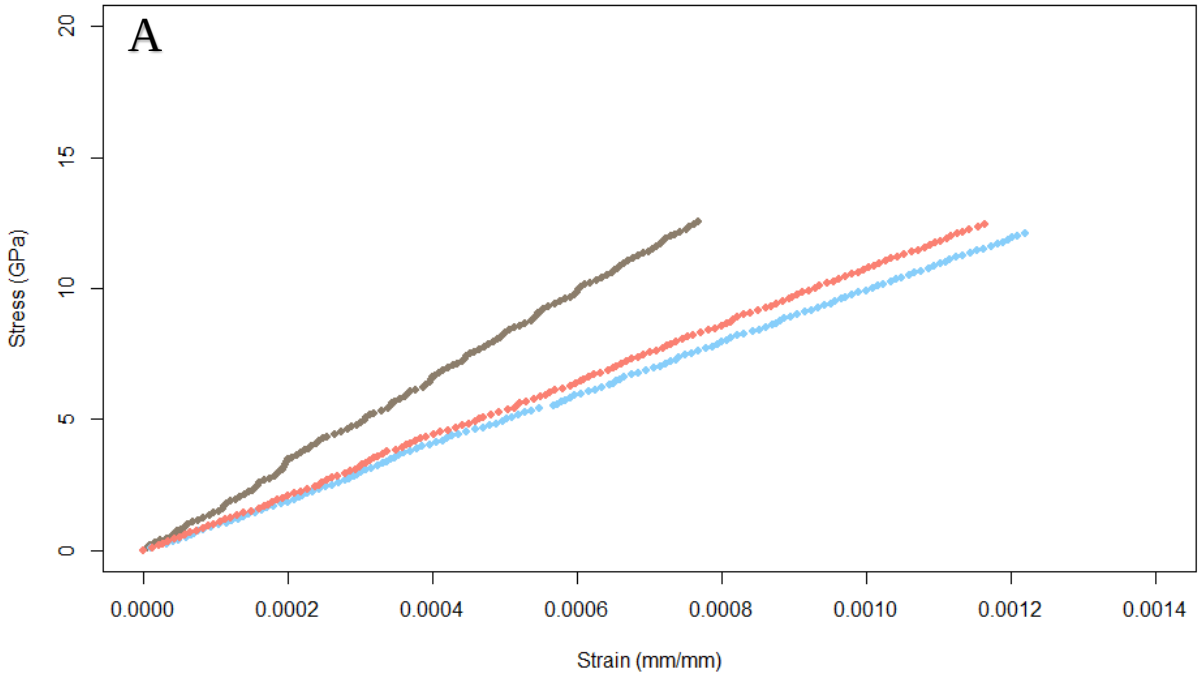

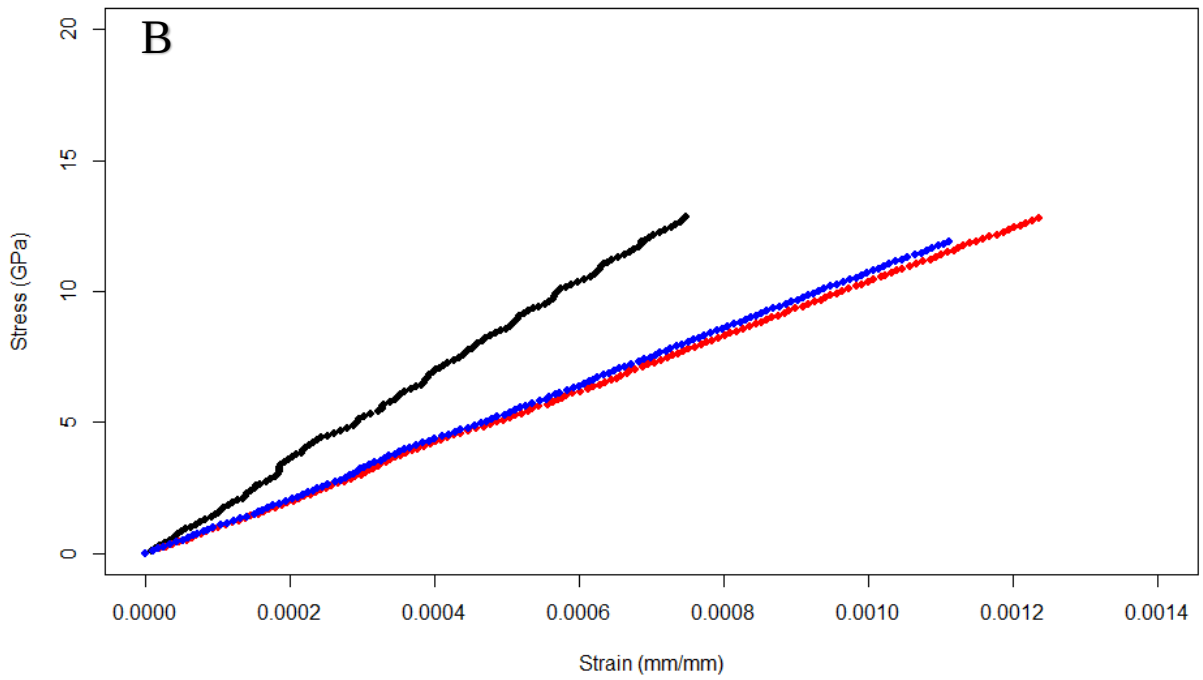

Figure 8. A) Average stress-strain curves for the cranial aspect of the humerus (n= 30) with colors representing each of the orthogonal directions tested (brown = axial, light red = radial and light blue = transverse) B) Average stress-strain curves for the caudal aspect of the humerus (n= 37) with colors representing each of the orthogonal directions tested (black = axial, red = radial and blue = transverse). Each curve was generated by averaging all stress-strain curves from the corresponding aspect of the bone (cranial or caudal) for a specific orientation, to obtain a single representative stress-strain curve. Bone cubes tested in the transverse and radial directions show non-significant differences in their stiffness values in both the cranial and caudal aspects, highlighting the transverse isotropic behavior of all the cubes tested

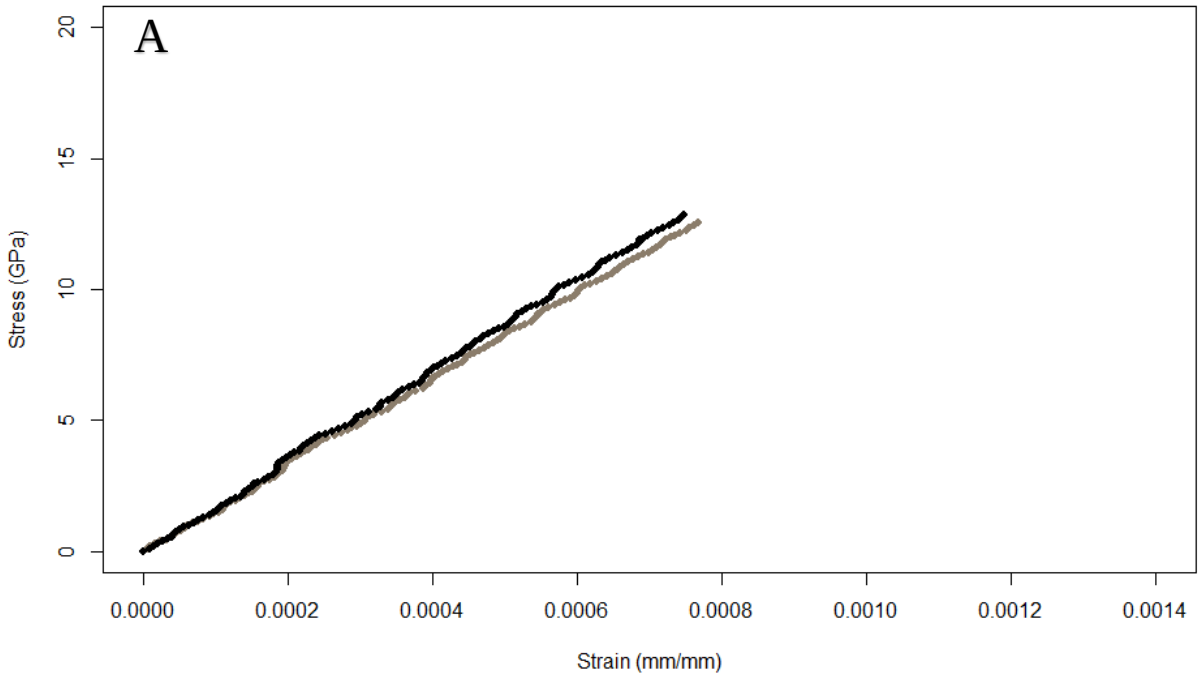
A
Stress (GPa)
0
5
10
15
20
0.0000
0.0002
0.0004
0.0006
0.0008
0.0010
0.0012
0.0014
Strain (mm/mm)

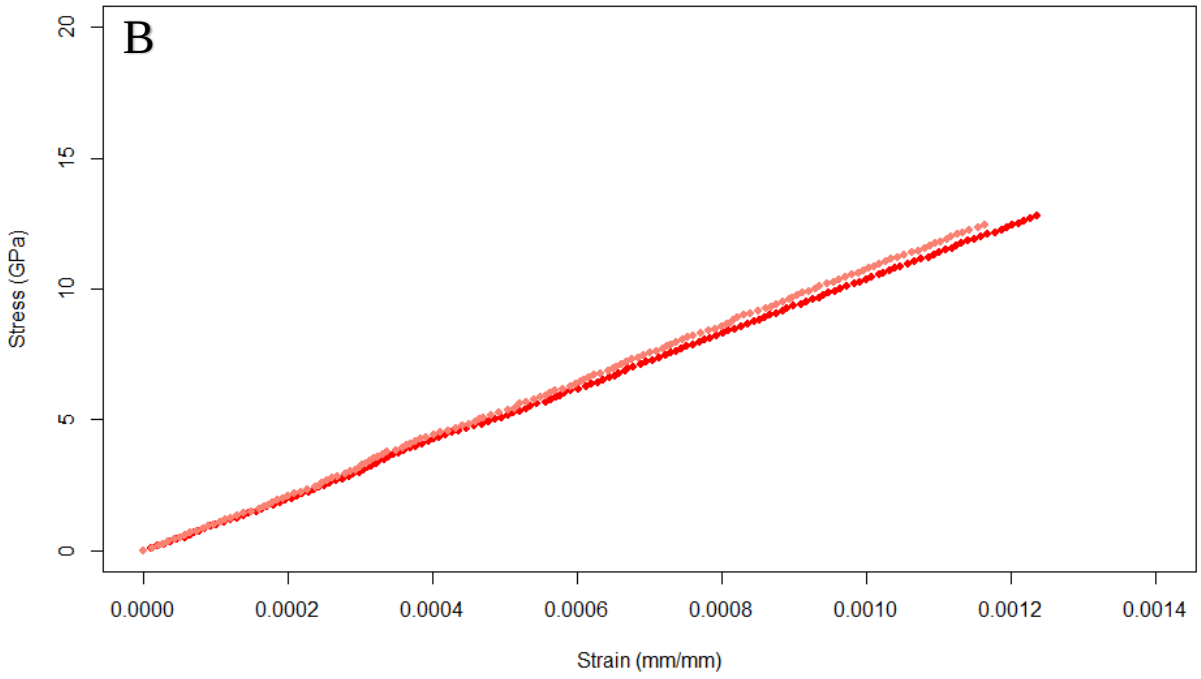
B
Stress (GPa)
0
5
10
15
20
0.0000
0.0002
0.0004
0.0006
0.0008
0.0010
0.0012
0.0014
Strain (mm/mm)

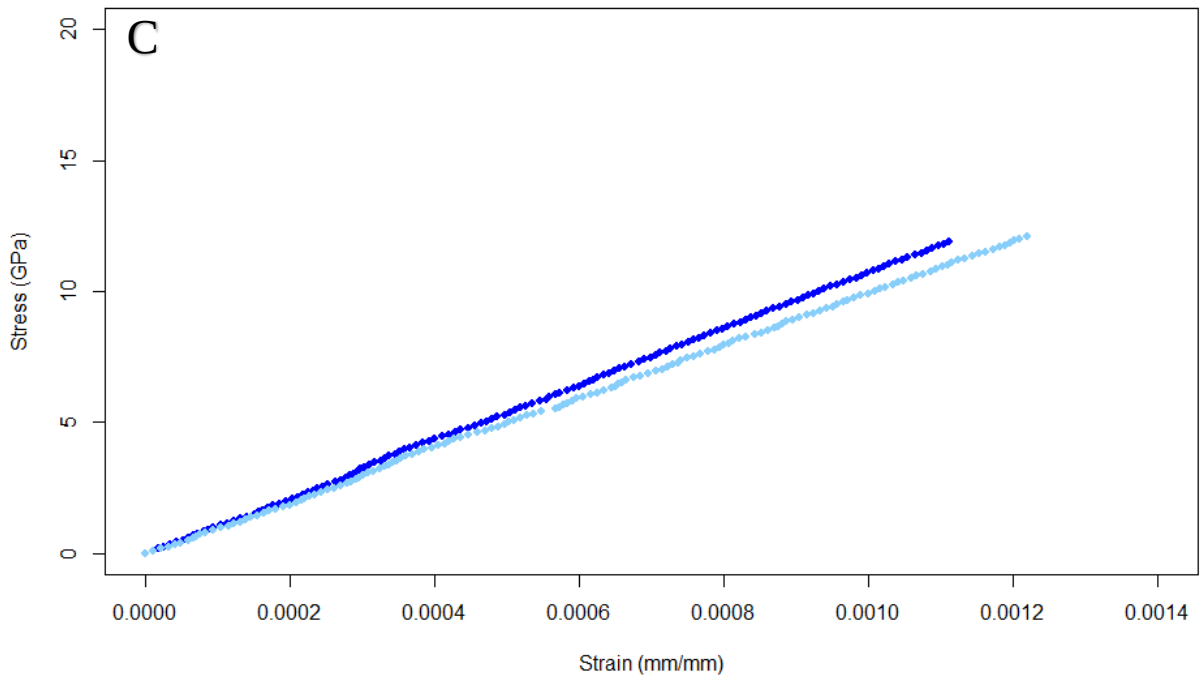

Figure 9. Average stress-strain curve comparing stiffness values for all cortical bone cubes from the cranial (n= 30) and caudal (n = 37) aspects of the proximal humerus when loaded in the axial direction (2A; cranial brown and caudal black), radial direction (2B; cranial light red and caudal red) and transverse direction (2C; cranial light blue and caudal blue). Bone cubes tested in all three directions showed no significant difference when comparing the cranial vs caudal aspects of the bone.

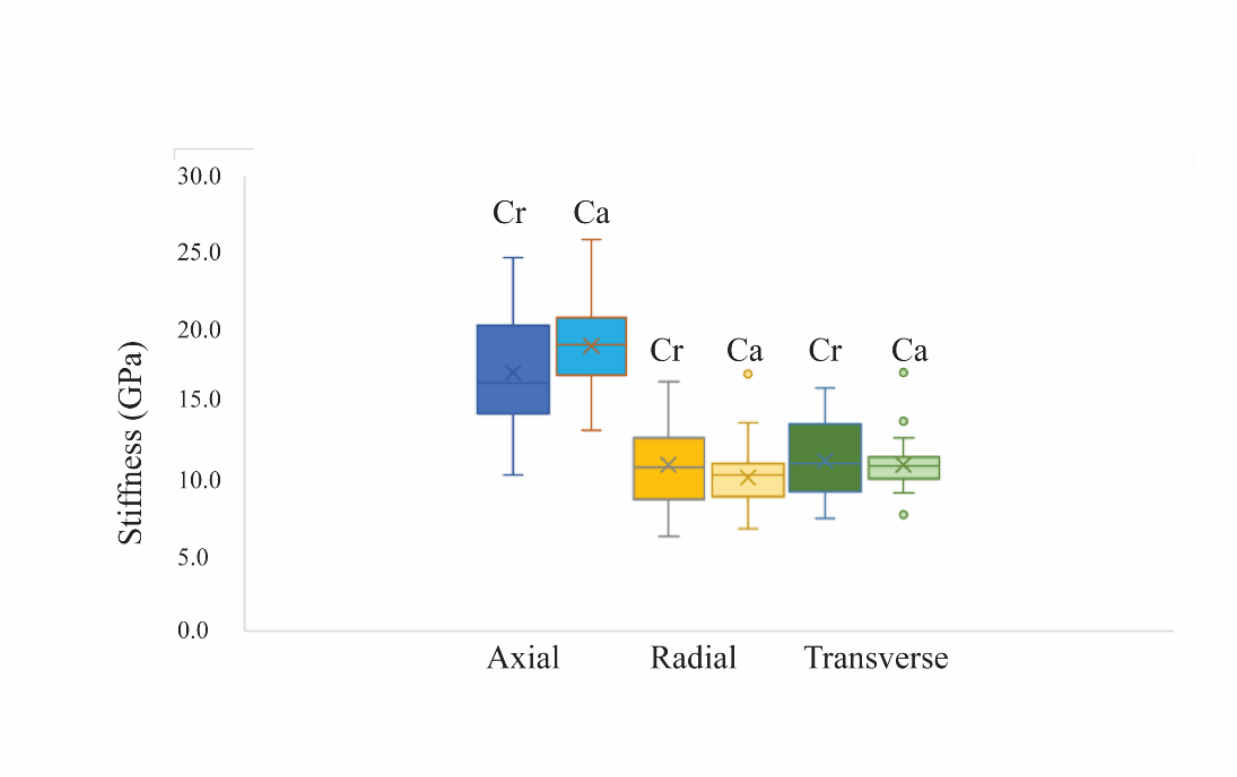

Figure 10. Box plot diagram comparing the stiffness values between cranial and caudal aspects. Cranial orientations were labeled as follows; dark blue = axial, dark yellow = radial, dark green = transverse. Caudal orientations are color-labeled as follows; light blue = axial, light yellow = radial, light green = transverse. Overall, there was no significant difference in compressive stiffness between the cranial and caudal aspects. The horizontal line within each box plot represents the median, 'X' represents the average. Hinges on all boxes represent 25th and 75th percentiles with whiskers indicating minimum and maximum measured values (excluding outliers). Outliers are represented by circles in the diagram and are defined as any data point that is located 1.5 times above the upper quartile or 1.5 times below the lower quartile.

Bone Material Composition

Mineral (hydroxyapatite), organic material and water were all found to be non-significantly different between the cranial and caudal aspects of the white-tailed deer proximal humerus (Figure 11). Mineral content was found to be 25.8% ± 1.2 and 24.8.7% ± 1.6 in the cranial and caudal aspects respectively. Organic material percentage (mostly collagen) was found to be 62.9% ± 2.0 and 63.7% ± 2.1 in the cranial and caudal aspects respectively. Water percentage was found to be 11.3% ± 2.4 and 11.5 ± 1.8 in the cranial and caudal aspects respectively. (Table 2).

	Cranial aspect Average (SD) %	Caudal aspect Average (SD) GPa
Mineral	25.8 (1.2)	24.8 (1.6)
Organic material	62.9 (2.0)	63.7 (2.1)
Water	11.3 (1.3)	11.5 (1.8)

Table 2. Average mineral, organic material and water percentage (standard deviation in parenthesis) for samples ashed from the cranial and caudal aspects of the proximal humerus in white-tailed deer.

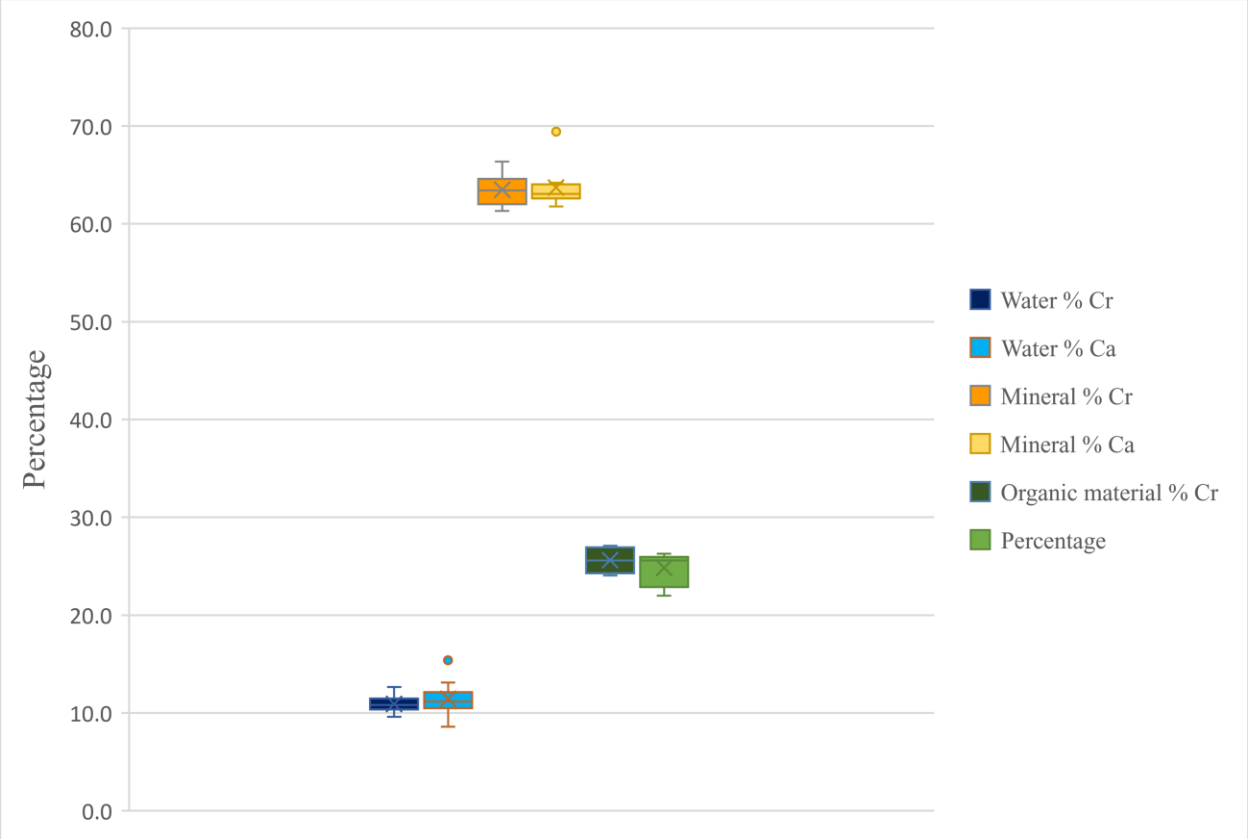

Figure 11. Box plot diagram showing mineral (hydroxyapatite), organic material (mostly collagen) and water percentage from cortical bone cubes ashing. There was no significant difference in mineral, organic material and water percentage when comparing cubes from the cranial and caudal aspects. The horizontal line within each box plot represents the median, 'X' represents the average. Hinges on all boxes represent 25th and 75th percentiles with whiskers indicating minimum and maximum measured values (excluding outliers). Outliers are represented by circles in the diagram and are defined as any data point that is located 1.5 times above the upper quartile or 1.5 times below the lower quartile.

Discussion

The data from my undergraduate research revealed that secondary osteons from the cranial aspect of the proximal humerus of white tailed deer (*Odocoileus virginianus*) were significantly larger and more angled medially when compared against secondary osteons from the caudal, medial, and lateral aspects (Figure 2A and 2B).

Previous studies have also shown that remodeling rate (number of secondary osteons in a given region over a period of time) as well as the shape and size of secondary osteons are affected by the type, magnitude, and frequency of loading (Layton et al., 1979; Martin et al., 1996; Keenan et al., 2017). A previous study by Skedros et al., (1994) examined the microstructure of secondary osteons in the tension and compression cortices of calcanei taken from mature mule deer. The calcanei of mule deer are simply loaded in tension/compression during locomotion; making them comparable to the humeri used in my study. Similar to my results, Skedros et al., (1994) observed significantly smaller osteons in the compression cortices (0.0016 mm^2 per osteon on average) compared to the tension cortices (.0022 mm^2 per osteon on average). In a study that compared secondary osteonal size and population density across various species, Skedros et al., (2012) demonstrated differences across regions that were subjected to diverse types of load. Their results showed a significantly greater number of secondary osteons between the tension and compression regions of deer and equine calcanei as well as sheep and equine radii. A significant difference in secondary osteonal size was also observed between the dorsal and plantar regions of deer and horse calcanei; the cranial and caudal regions of sheep radii; and the anterior and posterior regions of chimpanzee femora. In another study by Skedros

et al., (2003), similar differences were observed between secondary osteons in tension and compression regions in the calcanei of immature mule deer. Secondary osteons in the compression cortices were 35% smaller when compared against secondary osteons from the tension cortices.

A possible explanation for these size differences was proposed by (Skedros et al., 1997). Regions loaded primarily in tension (e.g. cranial aspect of the proximal humerus) experience generally lower stress magnitudes compared to regions that are loaded primarily in compression (e.g. caudal aspect of the proximal humerus). These higher stressed regions would benefit from smaller resorption pits (and thus smaller secondary osteons) as this would mean that less bone material is lost during each remodeling event. This smaller resorption pits were also predicted to correlate with a smaller decrease in bone stiffness and strength and a lesser chance for microcracks to form and a fractures to occur (Skedros et al., 1997).

Much less is known, however, about how secondary osteonal morphology and size affects bone mechanical properties. A study by Bernhard et al., (2013) attempted to quantify the effect of individual osteon morphology on the overall stability of the human femur in terms of its resistance to buckling, bending and compression. In this study, estimated resistance values were calculated based on the average diameter and area of secondary osteons in the proximal femur. However, this study did not perform any actual mechanical testing, so these values were only theoretical., A similar study by Li et al., (2013) attempted to correct for microstructural differences across regions of the bovine femur by applying Voigt-Reuss-Hill averaging scheme in order to approximate the

effective stiffness of the bone tissue. This scheme incorporates osteonal, interstitial, and plexiform areas of the bone in addition to their corresponding stiffness values (based on accepted values from the literature) in order to predict a single overall stiffness value for the cortical bone tissue. Similar to the previous study (Bernhard et al., 2013) this value only provides an estimate of the mechanical properties of the tissue and is not based on actual testing.

Given the lack of data on the relationship between secondary osteon morphology and compressive stiffness, the aim of my graduate research was to determine whether differences in secondary osteonal size and morphology (angle of orientation) between the cranial and caudal aspects of the proximal humerus of white-tailed deer affected the stiffness of those regions. I hypothesized that cortical bone samples containing smaller secondary osteons from the caudal aspect (subjected to higher compressive stresses) would have significantly higher stiffness values for the axial, radial, and transverse directions compared to cortical bone samples containing larger secondary osteons from the cranial aspect (subjected to lower tensile stresses).

Bone cubes from the cranial and caudal aspects of the proximal humerus tested in compression along their axial direction demonstrated an average stiffness of 17.2 ± 4.2 GPa and 18.5 ± 3.2 GPa for cranial and caudal aspects respectively. These values are within the range of previously reported values of 18.7 ± 2.8 GPa (cranial) and 15.33 ± 2.8 GPa (caudal) for samples taken from equine radii (Riggs et al., 1993). Bone cubes tested along their radial direction demonstrated an average stiffness of 10.7 ± 2.4 GPa and 10. ± 2.1 GPa for the cranial and caudal aspects respectively. These values are within the range of

predicted radial stiffness values of 13.0 GPa and 9.0 GPa for the cranial and caudal aspects of the human femur respectively (Li et al., 2013). Bone cubes tested along their transverse direction demonstrated an average stiffness of 11.0 ± 2.4 GPa and 10.9 ± 1.8 GPa for cranial and caudal aspects respectively. These values are within the range of previously reported transverse stiffness values of 10.4 ± 1.64 to 13.0 ± 4.62 GPa for the cranial aspect and 10.1 ± 1.78 GPa to 22.3 ± 3.18 GPa for the caudal aspect of bovine femora (Reilly and Burstein 1975).

Previous studies by Barrera et al., (2016) and Kunde et al., (2018) have used cortical bone samples taken from the same young white-tailed deer, yet their studies reported orthotropic stiffness values for the axial, radial, and transverse orientations which were higher than my results. Barrera et al., noted stiffness values of 21.6 ± 3.3, 17.6 ± 3.0 and 14.9 ± 1.9 GPa for the axial, transverse and radial orientations respectively, while Kunde et al., reported the stiffness of the axial, transverse and radial orientations to be 24.4 ± 4.4 GPa, 16.8 ± 3.3 GPa and 14.6 ± 2.8 GPa respectively. The discrepancy between the results of these studies and mine can be attributed to regional differences in the samples. Kunde et al., used samples from the mid-diaphysis of the humerus whereas Barrera et al used samples from the proximal femur. These regions in comparison to the proximal humerus were not as remodeled. Therefore, samples taken from these regions contained mostly primary bone whereas the samples from my study had mainly secondary or osteonal bone. Primary bone is more mineralized and different in its structure and thus displays the orthotropic behavior observed in those previous studies, whereas secondary bone is less mineralized and displays the transverse-isotropic behavior shown in my study.

The differences in stiffness values between the current study and the literature are not surprising given the use of various animal and bones. In addition, while previous studies have used mostly adult animals, all the cortical bone samples in my study were from young deer whose bones were not highly mineralized. Mineral content (by weight) was found to be 63.5% ± 2.0% and 63.7% ± 2.1% and organic material content (by weight) was found to be 25.6% ± 1.2% and 24.8.7% ± 1.6% for the cranial and caudal aspects respectively. In contrast, average mineral content of adult mammals was reported in the literature to be around 70% (Driessens and Verbeeck, 1990). This difference in mineralization can explain the lower stiffness values observed in my study, as the increased mineral percentage in adult animals (mineral accumulates and replaces water) has been shown to result in stiffer bone tissue overall.

Overall, the mechanical testing results refute my hypothesis, as no significant difference in stiffness was found for any direction of loading when comparing the cranial and caudal aspects. The largest (although not statistically significant) difference in stiffness values was found in the axial direction (17.2 ± 4.2 GPa and 18.5 ± 3.2 GPa for the cranial and caudal aspects respectively). As this is the direction that normally corresponds to physiological loading, the lack of a significant difference in stiffness between the cranial and caudal aspects of the proximal humerus is a clear indication that the morphological differences created during the resorption phase of remodeling (i.e. the size and shape of resorption pits created by osteoclasts) are independent from the material properties of the new bone material deposited during the formation phase of remodeling (i.e. mineral, collagen and water content in new bone deposited by osteoblasts). While my undergraduate research showed a significant difference in secondary osteon size, my current study shows

no significant difference in the amount of mineralization (hydroxyapatite) between the cranial and caudal aspects. The mineral portion of bone is one of the main components of bone material and has been shown to have a significant contribution to its mechanical properties such as strength and stiffness (Schaffler and Burr, 1988). In conclusion, the combined results showed that while secondary osteons in the cranial and caudal aspects differ morphologically in terms of size, orientation; they have the same mineral content and thus their compressive stiffness does not differ.

An expected finding of this study was the transverse isotropic mechanical behavior of the cortical bone cubes tested in both the cranial and caudal aspects of the proximal humerus. Average stiffness values in the radial and transverse directions of the cranial aspect were 10.7 ± 2.4 GPa and 11.0 ± 2.4 GPa respectively. Average stiffness values in the radial and transverse directions of the caudal aspect were 10. ± 2.1 GPa and 10.9 ± 1.8 GPa respectively. This isotropic behavior is directly related to the extent of remodeling observed in all the samples. When examining the SEM images and the paraffin-embedded sections, the extent of bone remodeling and the predominantly presence of secondary osteons is clearly shown (Figures 1 and 6). This finding indicates that these samples consist of secondary osteons organized normal to the transverse-radial plane and parallel to the axial axis. This observation is consistent with previous studies which noted that secondary osteons are preferentially oriented along the long axis of the bone (Lanyon et al., 1979). Human osteonal bone has also been noted as being transverse isotropic (Reilly and Burstein 1975).

My hypothesis for this study was based on previous research which noted that humerus and other bones associated with the forelimbs in deer such as the radius,

metacarpal and phalanx are believed to function similarly to beams loaded in bending with corresponding regions being subjected primarily to tension and compression (Skedros et al., 2012). However, a recent study suggested this may be an oversimplification, as the cranial cortex of the deer calcaneus (originally believed to be loaded primarily in tension) was shown to be affected mostly by shear strains when taking into account max shear data (Skedros et al., 2019). This addresses a potential limitation with this study, as I only tested samples in compression. A different testing method, such as 3-point bending or even a computer model (Finite Element Analysis), may better account for the shear stresses across the cranial and caudal aspects of the humerus. In addition, I did not measure and compare the strength (maximum stress) between the cranial and caudal aspects of the proximal humerus as the universal testing machine (Instron 5942) is incapable of reaching these high stresses. Differences in osteon morphology may affect the bone's resistance to failure in ways that were not explored in this study.

In summary, I measured cortical bone stiffness from the proximal humerus of white-tailed deer in all three orthogonal directions and observed no significant difference for any direction when comparing samples from the cranial and caudal aspects. Samples from both aspects showed transverse isotropic behavior, which is consistent with the secondary osteonal bone present. Stiffness values from this study were generally lower than previously reported values which can be attributed to the young age of the animals and the lower mineral content of their bones. In addition, the mineral content was also not significantly different between the cranial and caudal aspects. This supports the mechanical testing data as samples from both cranial and caudal aspects were shown to be similar in their material properties and therefore are expected to display similar mechanical

properties. In conclusion, the null hypothesis for this experiment was supported, as there was no observed difference in the stiffness or mineralization when comparing the cranial and caudal aspects of the proximal humerus. These findings, in addition to the results from my undergraduate research suggest that the compressive stiffness of the cranial and caudal aspects do not differ based on secondary osteon size or morphology. These findings also indicate that the resorption and formation phases of bone remodeling (governed by osteoclasts and osteoblasts respectively) are independent from each other in regard to the effects of stress direction (compression or tension) and magnitude.

References

Allen MR, Burr DB (2014) Bone modeling and remodeling. In: Basic and Applied Bone Biology. (Burr D, Allen M, eds) 1st Ed. Elsevier. pp. 75-90

Barak MM, Weiner S, Shahar R (2008) Importance of the integrity of trabecular bone to the relationship between load and deformation of rat femora: An optical metrology study. *Journal of Materials Chemistry* 18: 3855-3864

Barak MM, JD Currey, Weiner S, Shahar R. (2009) Are tensile and compressive Young's moduli of compact bone different? *Journal of the Mechanical Behavior of Biomedical Materials*. 2: 51-60

Barrera JW, Le Cabec A, Barak MM. (2016) The orthotropic elastic properties of fibrolamellar bone tissue in juvenile white-tailed deer femora. *Journal of Anatomy*. 229: 568-576

Bernhard A, Milovanovic P, Zimmerman EA, Hahn M, Djonic D, Krause M, Breer S, Puschel K, Djuric M, Amling M, Busse B (2013) Micro-morphological properties of osteons reveal changes in cortical bone stability during aging, osteoporosis, and bisphosphonate treatment in women. *Osteoporosis International*. 24: 2671-2680

Bonucci E. (2000) Chapter 1: Basic composition and structure of bone. In: Mechanical testing of bone and the bone-implant interface. (An YH, Draughn RA, eds) CRC Press. pp. 3-21

Buckwalter JA, Glimcher RR, Cooper R, Recker R. (1995) Bone Biology. *Journal of Bone and Joint Surgery*. 77: 1256-1275

Currey JD (1969) The Relationship Between the Stiffness and Mineral Content of Bone. *Journal of Biomechanics.* 2: 477-480

Currey JD. (2002) Chapter 1: The structure of bone tissue. In: Bones, structure and mechanics. Princeton: Princeton University Press. pp. 3-25

Dechow PC, Nail GA, Schwartz-Dabney CL, Ashman RB (1993) Elastic Properties of Human Supraorbital and Mandibular Bone. *American Journal of Physical Anthropology*. 90: 291-306

Ding M, Danielsen, CC, Hvid, I, Overgaard, S (2012) Three-dimensional microarchitecture of adolescent cancellous bone. *Bone*. 51: 953–960.

Dominguez VM, Crowder CM. (2012) The utility of osteon shape and circularity for differentiating human and non-Human Haversian bone. *American Journal of Physical Anthropology* 149(1): 84-91

Driessens FCM, Verbeeck RMH (1990) Biominerals. CRC Press. p. 180

Hadjidakis DJ, Androulakis II. (2007). Bone Remodeling. *Women's Health and Disease: Gynecologic, Endocrine, and Reproductive Issues*. 1092(1): 385-396

Keenan KE, Mears CS, Skedros JG. (2017) Utility of osteon circularity for determining species and interpreting load history in primates and nonpriamtes. *American Journal of Physical Anthropology*. 162(4): 657-681

Kunde AN, Frost VJ, Barak MM. (2018) Acute exposure of white-tailed deer cortical bone to Staphylococcus aureus did not result in reduced bone stiffness. *Journal of the Mechanical Behavior of Biomedical Materials*. 82: 329-337

Lanyon LE, Magee PT, Baggott DG. (1979) The relationship of functional stress and strain to the process of bone remodeling. An experimental study on the sheep radius. *Journal of Biomechanics*. 12: 593-600

Linde F, Hvid I (1999) Nondestructive mechanical testing of cancellous bone. In: Mechanical testing of bone and the bone implant interface. (An Yh, Draughn RA, eds) CRC Press. p. 154

Li S, Emrah D, Silberschmidt VV (2013) Variability and anisotropy of mechanical behavior of cortical bone in tension and compression. *Journal of the Mechanical Behavior of Biomedical Materials*. 21: 109-120

Martin RB, Gibson VA, Stover SM, Gibeling JC, Griffin LV (1996) Osteonal Structure in the Equine Third Metacarpus. *Bone*. 19(2): 165-171

Morgan EF, Bouxsein ML. (2008) Biomechanics of bone and age-related fractures. In:Principles of Bone Biology. Bilezikian JP, Raisz LG, Martin J, eds) 3rd Ed. San Diego: Academic Press. pp. 29-51

Morgan EF, Unnikrisnan GU, Hussein AI. (2018). Bone Mechanical Proeprties in Healthy and Diseased States. *Annual Review of Biomedical Engineering*. 20: 119-143

Ott SM (2018) Cortical or Trabecular Bone: What's the Difference? *American Journal of Nephrology*. 47: 373-375

Patterson-Kane JC, Firth EC (2013) Chapter 13: Tendon, Ligament, Bone, and Cartilage: Anatomy, Physiology, and Adaptations to Exercise Training. In: The Athletic Horse: Principles and Practice of Equine Sports Medicine. 2nd Ed. Saunders. pp.1-41

Porter A, Irwin R, Miller J, Horan DJ, Robling AG, McCabe LR (2017) Quick and inexpensive paraffin-embedding method for dynamic bone formation analyses. *Scientific Reports*. 7: 42505

Prafitt A.M (1994) Osteonal and Hemi-Osteonal Remodeling: The Spatial and Temporal Framework for Signal Traffic in Adult Human Bone. *Journal of Cellular Biochemistry*. 55: 273-286

Raggatt LJ, Patridge NC (2010) Cellular and Molecular Mechanisms of Bone Remodeling. The *Journal of Biological Chemistry*. 285(33): 25103-25018

Riggs CM, Vaughan LC, Evans GP, Lanyon LE, Boyde A. (1993) Mechanical implications of collagen fibre orientation in cortical bone of the equine radius. *Anatomy and Embryology*. 187: 239-248

Schaffler MB, Burr DB (1988) Stiffness of Compact Bone: Effects of Porosity and Density. *Journal of Biomechanics*. 21(1): 13-16

Sedlin ED ( ) Mechanical properties of bone. *Acta Orthopedica Scandinavica*. 83: 1

Sedlin ED, Hirsch C. (1966). Factors affecting the determination of the physical properties of femoral cortical bone. *Acta orthop. scandinav*. 37:29-48

Shahar R, Zaslansky P, Barak M, Friesem AA, Currey JD, Weiner S (2007) Anisotropic Poisson's ratio and compression modulus of cortical bone determined by speckle interferometry. *Journal of Biomechanics*. 40: 252-264

Sharir A, Barak MM, Shahar R (2008) Whole bone mechanics and mechanical testing. *The Veterinary Journal*. 177: 8-17

Skedros JG, Mason MW, Bloebaum RD (1994) Differences in Osteonal Micromorphology Between Tension and Compression Cortices of a Bending Skeletal System Indicative of Potential Strain-Specific Differences in Bone Microstructure. *The Anatomical Record*. 239: 405-413

Skedros JG, Mason MW, Nelson MC, Bloebaum RD (1996) Evidence of Structural and Material Adaptation to Specific Strain Features in Cortical Bone. *The Anatomical Record*. 246: 47-63

Skedros JG, Su CS, Bloebaum RD. (1997) Biomechanical Implications of Mineral Content and Microstructural Variations in Cortical Bone of Horse, Elk, and Sheep Calcanei. *The Anatomical Record*. 249: 297-316

Skedros JG, Mason MW, Bloebaum RD (2001) Modeling and Remodeling in a Developing Artiodactyl Calcaneus: A Model for Evaluating Frost's Mechanostat Hypothesis and Its Corollaries. *The Anatomical Record* 263: 167-185

Skedros JG, Sybrowsky CL, Parry TR, Bloebaum RD (2003) Regional Differences in Cortical Bone Organization and Microdamage Prevalence in Rocky Mountain Mule Deer. *The Anatomical Record*. 274A: 837-850

Skedros JG, Sorenson SM, Jenson NH (2007) Are Distributions of Secondary Osteon Variants Useful for Interpreting Load History in Mammalian Bones. *Cells Tissues Organs*. 185: 285-307

Skedros JG, Mendenhall SD, Kiser CJ, Winet H. (2009) Interpreting cortical bone adaptation and load history by quantifying osteon morphotypes in circularly polarized light images. *Bone*. 44: 392-403

Skedros JG. (2011). Chapter 7: Interpreting Load History in Limb-Bone Diaphyses: Important Considerations and Their Biomechanical Foundations. In: Bone Histology: An Anthropological Perspective. (Crowder C, Stout S, eds) CRC Press. pp.153-220

Skedros JG, Keenan KE, Williams TJ, Kiser CJ. (2013) Secondary osteon size and collagen/lamellar organization (‘‘osteon morphotypes’’) are not coupled, but potentially adapt independently for local strain mode or magnitude. *Journal of Structural Biology*. 181: 95-107

Skedros JG, Su SC, Knight AN, Bloebaum RD Bachus KN (2019) Advancing the deer calcaneus model for bone adaptation studies: ex vivo strains obtained after transecting the tension members suggest an unrecognized important role for shear strains. *Journal of Anatomy*. 234: 66-82

Teitelbaum SL (2000) Bone Resorption by Osteoclasts. *Science*. 289: 1504-1507

Timmins PA, Wall JC. (1977) Bone water. *Calcified Tissue Research*. 23: 1-5

Turner CH, Burr DB. (1993) Basic Biomechanical Measurements of Bone: A Tutorial., *Bone*. 14: 595-608

Zioupos P, Currey JD (1998) Changes in the stiffness, strength, and toughness of human cortical bone with age. *Bone*. 22(1): 57-66